Journal of Solid Mechanics Vol. 11, No. 4 (2019) pp. 690-706
DOI: 10.22034/jsm.2019.668608

Analysis of Viscoelastic Functionally Graded Sandwich Plates with CNT Reinforced Composite Face Sheets on Viscoelastic Foundation

A. GhorbanpourArani [1,2 *], M. Emdadi [2], H. Ashrafi [2], M. Mohammadimehr [2], S.Niknejad [2], A.A. Ghorbanpour Arani[3], A. Hosseinpour [4]

[1]*Institute of Nanoscience & Nanotechnology, University of Kashan, Kashan, Iran*
[2]*Department of Solid Mechanics ,Faculty of Mechanical Engineering, University of Kashan, Kashan , Iran*
[3]*School of Mechnical Engineering, College of Engineering, University of Tehran, Tehran, Iran*
[4]*Department of Mechanical Engineering and Engineering Science, University of North Carolina at Charlotte, USA*

Received 30 June 2019; accepted 30 August 2019

ABSTRACT

In this article, bending, buckling, and free vibration of viscoelastic sandwich plate with carbon nanotubes reinforced composite facesheets and an isotropic homogeneous core on viscoelastic foundation are presented using a new first order shear deformation theory. According to this theory, the number of unknown's parameters and governing equations are reduced and also the using of shear correction factor is not necessary because the transverse shear stresses are directly computed from the transverse shear forces by using equilibrium equations. The governing equations obtained using Hamilton's principle is solved for a rectangular viscoelastic sandwich plate. The effects of the main parameters on the vibration characteristics of the viscoelastic sandwich plates are also elucidated. The results show that the frequency significantly decreases with using foundation and increasing the viscoelastic structural damping coefficient as well as the damping coefficient of materials and foundation.

Keywords: Viscoelastic sandwich plate; Carbon nanotube reinforcement; New first order shear deformation theory; Bending; Buckling; Free vibration.

1 INTRODUCTION

IN recent years, Composite sandwich structures are widely used in the field of transportation (helicopter blades, ship's hull, etc.), urban services, and any other fields due to their low specific weight, bending rigidity, excellent vibration characteristics and good fatigue properties [1]. Sandwich construction has become even more attractive to the introduction of advanced composite materials for the face sheets, e.g. fiber reinforced composites especially carbon nanotubes (CNTs) reinforced composite facesheets. Experimental investigations show that CNTs have

*Corresponding author. Tel.: +98 31 55912450; Fax: +98 31 55912424.
E-mail address: aghorban@kashanu.ac.ir (A. Ghorbanpour Arani).

extraordinary mechanical properties over carbon fibers [2-3]. Thereby, to improve the characteristics, the face sheets can be laminated composites [4], functionally graded materials [5] or polymer matrix with reinforcements [6]. Thostenson and Chou [7] showed that the addition of nanotubes increases the tensile modulus, yield strength and ultimate strengths of the polymer films. Their study has also showed that the polymer films with aligned nanotubes as reinforcements yield superior strength to randomly oriented nanotubes. Moreover, Zhu et al., [8] studied the static and free vibration of CNT reinforced plates based on the first-order shear deformation theory. They considered polymer matrix with CNT reinforcement. It was predicted that the CNT volume fraction has greater influence on the fundamental frequency and the maximum center deflection. Mohammadimehr et al., [9], considered biaxial buckling and bending of smart nanocomposite plate reinforced by CNT using extended mixture rule approach. It was shown that nonlocal deflection of smart nanocomposite plate decreases with an increase in the magnetic field intensity and the stability of smart nanocomposite plate increases in the presence of elastic foundation. Ghorbanpour et al., [10], studied the buckling and post-buckling characteristics of CNT reinforced plates using the finite element method. It was shown that the reinforcement with CNT increasing the load carrying capacity of the plate. Ghorbanpour et al., [11], used DQM for Nonlinear vibration analysis of laminated composite Mindlin micro/nano-plates resting on orthotropic Pasternak medium, they showed that considering elastic medium increases the nonlinear frequency of system and the effect of boundary conditions becomes lower at higher nonlocal parameters. While the shear deformation effect is more practical in thick plates or plates made of advanced composites, shear deformation theories such as first-order shear deformation theory (FSDT) and higher-order shear deformation theories (HSDT) should be used to anticipate the responses of FG sandwich plates. The FSDT needs to the shear correction factor for determining acceptable results but it is hard to determine and it depends on many parameters. Conversely, the HSDT do not require shear correction factor, but its equations of motion are more complicated than those of FSDTs. Zenkour and Sobhy [12] used FSDT, SSDT and third-order shear deformation theory (TSDT) for Thermal buckling of various types of FGM sandwich plates. They considered the effects of the gradient index, loading type and sandwich plate type on the critical buckling for sandwich plates. Sobhy [13] investigated buckling and free vibration of exponentially graded sandwich plates resting on elastic foundations under various boundary conditions.

He considered the effect of the inhomogeneity parameter, and the foundation parameters on the natural frequencies and critical buckling loads. Based on the new first-order shear deformation theory, Huu-Tai Thai et al., [14], considered the analysis of functionally graded sandwich plates. They showed that the new first-order shear deformation theory is not only more accurate than the conventional one, but also comparable with higher-order shear deformation theories which have a greater number of unknown parameters. Inspired by the concept of functionally graded materials (FGMs), researchers adopted the functionally graded (FG) pattern of reinforcement for FG–CNT reinforced composite plates in their study. Zhang et al., [15] considered an element-free IMLS-Ritz framework for buckling analysis of FG–CNT reinforced composite thick plates resting on Winkler foundations. It is found that FG–CNT reinforced composite plates with top and bottom surfaces of CNT-rich have the highest critical buckling loads. Shen [16] studied the nonlinear bending of FG–CNT reinforced composite plates in thermal environment. He found that the load bending moment curves of the plates could be considerably improved through the use of a functionally graded distribution of CNTs in the matrix. Moreover, kp-Ritz method has been utilized to study the dynamic stability, large deflection, buckling and post buckling behaviors of FG–CNT reinforced composite plates and panels [17-20]. It should be observed that a large amount of previous researches have been concentrated on the computation of statics analysis of sandwich plates surrounded with elastic medium. In some proposed applications of sandwich plates such as FG–CNT reinforced composite plates and panels, the nanoplates are embedded in polymer that is depicted viscoelastic property [21]. Generally, in a viscoelastic medium, a part of deformation energy is recoverable and the other part is irrecoverable. Thus, the vibration analysis in viscoelastic medium has to pay more attention to elastic medium.

Moreover, in the available articles, nano sandwich plates are modeled as elastic plates whereas they similar to many materials reveal viscoelastic structural damping. Su et al. [22] studied on viscoelastic properties of graphene oxide nano-plate experimentally. Pouresmaeeli et al., [23] considered vibration analysis of viscoelastic orthotropic nanoplates resting on viscoelastic medium. They showed that the frequency significantly decreases with increasing the structural damping coefficient as well as the damping coefficient of foundation.

In this paper, a new FSDT which eliminated the shear correction factor and reduced the number of unknown and governing equation is used for viscoelastic functionally graded sandwich plates with CNT reinforced composite facesheets by considering of viscoelastic foundation. The viscoelastic medium such as polymer matrix and foundation is obtained as Kelvin–Voigt model. Equations of motion and boundary conditions are derived from Hamilton's principle. Analytical solutions for rectangular plates under various boundary conditions are obtained. Thus, the result of bending, buckling, and free vibration that is considered in viscoelastic medium is compared with them in elastic medium.

2 THEORETICAL FORMULATION

Consider a rectangular sandwich plate composed of three layers as shown in Fig. 1. We assume that the CNT reinforced layers as top and bottom facesheets are made from a mixture of single walled CNT, graded distribution in the thickness direction and the matrix is assumed to be isotropic, while a core is made of an isotropic homogeneous material as a middle layer. The core-to-facesheet thickness ratio is h_c / h_f , where, h_c is the core thickness and h_f is the facesheet thickness. The length and the width of the plate are *a* and *b* in *X* and *Y* direction, respectively.

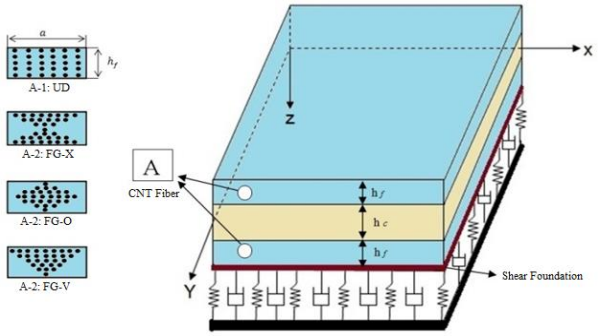

Fig.1
Geometry of viscoelastic sandwich plate on viscoelastic foundation with different functionally graded distribution of CNTs in the facesheets.

The effective properties of reinforced structures can be used by Mori-Tanaka scheme [9] or by the rule of mixtures. In this article, we use simple rule of mixtures with correction factors to estimate the effective material properties of CNT reinforced matrix. The effective material properties of the CNT reinforced matrix are given by [24]:

$$
\begin{aligned}
&E_{11} = \eta_1 V_{CNT} E_{11}^{CNT} + V_m E_m \\
&\frac{\eta_2}{E_{22}} = \frac{V_{CNT}}{E_{22}^{CNT}} + \frac{V_m}{E_m} \\
&\frac{\eta_3}{G_{12}} = \frac{V_{CNT}}{G_{12}^{CNT}} + \frac{V_m}{G_m} \\
&v_{12}^{CNT} = v_{12}^{CNT} V_{CNT} + v_m V_m \\
&\rho = \rho_{CNT} V_{CNT} + \rho_m V_m
\end{aligned}
\tag{1}
$$

where E_{11}, E_{22} and G_{12} are the Young's moduli and the shear modulus of the CNT, and V_{CNT} and V_m are the volume fraction of the CNT and the matrix, respectively.

The volumes fractions are related by $V_{CNT} + V_m = 1$. η_1, η_2 and η_3 are the efficiency of the inconsistency in the load transfer between CNT and matrix. The sandwich plate is made up of a homogeneous core with core thickness h_c and two facesheets with thickness h_f . The facesheets are supposed to be reinforced with CNTs. We suppose the volume fraction V_{CNT} for the top facesheet as:

$$
V_{CNT} = 2\left(\frac{t_1 - z}{t_1 - t_0}\right) V_{CNT}^{*} \tag{2}
$$

and for the bottom facesheet as:

$$
V_{CNT} = 2\left(\frac{z - t_2}{t_3 - t_2}\right) V_{CNT}^{*} \tag{3}
$$

where

$$V^{*}_{CNT} = \frac{w_{CNT}}{w_{CNT} + \left(\frac{\rho_{CNT}}{\rho_m}\right)(1 - w_{CNT})} \tag{4}$$

w_{CNT} is the mass fraction of the nanotubes. ρ_{CNT} and ρ_m are the mass densities of carbon nanotube and the matrix, respectively. The CNTs are either uniformly distributed or functionally graded along the thickness direction according to three cases of *FG-V, FG-O*, and *FG-X* types, given by [25]:

$$V_{CNT}(z) = \begin{Bmatrix} V^{*}_{CN} & UD \\ \left(1 + \frac{2z}{h}\right) V^{*}_{CNT} & FG-V \\ 2\left(1 - \frac{2|z|}{h}\right) V^{*}_{CNT} & FG-O \\ 2\left(\frac{2|z|}{h}\right) V^{*}_{CNT} & FG-X \end{Bmatrix} \tag{5}$$

Note that the case corresponds to the uniformly distributed CNT layers referred to as UD. It is assumed that the mass fraction of the CNTs (w_{CNT}) is the same in all cases.

2.1 Kinematics equation of sandwich plate

The displacement field of the conventional FSDT is given by:

$$\begin{aligned} u_1(x, y, z) &= u(x, y) + z\,\varphi_x(x, y) \\ u_2(x, y, z) &= v(x, y) + z\,\varphi_y(x, y) \\ u_3(x, y, z) &= w(x, y) \end{aligned} \tag{6}$$

where u, v, and w are displacement functions of the mid-plane of the plate in x, y, and z direction. By assuming $\varphi_x = -\partial w/\partial x$ and $\varphi_y = -\partial w/\partial y$ displacement field could be converted to CLP but by defining $\varphi_x = -\partial\theta/\partial x$ and $\varphi_y = -\partial\theta/\partial y$ as a new unknown parameter the displacement field of the new FSDT can be rewritten in form as:

$$\begin{aligned} u_1(x, y, z) &= u(x, y) - z\,\frac{\partial\theta}{\partial x} \\ u_2(x, y, z) &= v(x, y) - z\,\frac{\partial\theta}{\partial y} \\ u_3(x, y, z) &= w(x, y) \end{aligned} \tag{7}$$

As it is shown in Eq. (6) there are four unknown parameter (u, v, w, θ) instead of five. Therefore, the displacement field and subsequent equations of motion will be completely different with simple FSDT. In addition, the present FSDT does not require a shear correction factor because the transverse shear stresses are directly computed from the transverse shear forces by using equilibrium equations. The strain–displacement relations in Eq. (6) are:

$$\begin{Bmatrix} \varepsilon_x \\ \varepsilon_y \\ \gamma_{xy} \end{Bmatrix} = \begin{Bmatrix} \varepsilon^0_x \\ \varepsilon^0_y \\ \gamma_{xy} \end{Bmatrix} + z \begin{Bmatrix} \kappa_x \\ \kappa_y \\ \kappa_{xy} \end{Bmatrix} \qquad \begin{Bmatrix} \gamma_{xz} \\ \gamma_{yz} \end{Bmatrix} = \begin{Bmatrix} \gamma^0_{xz} \\ \gamma^0_{yz} \end{Bmatrix} \tag{8}$$

Eq. (7) can be rewritten in a compact form as:

$$\begin{aligned}\{\varepsilon\} &= \{\varepsilon^0\} + z\,\{\kappa\} \\ \{\gamma\} &= \{\gamma^0\}\end{aligned} \tag{9}$$

where

$$\{\varepsilon^0\} = \begin{Bmatrix}\varepsilon_x^0 \\ \varepsilon_y^0 \\ \gamma_{xy}^0\end{Bmatrix} = \begin{Bmatrix}\dfrac{\partial u}{\partial x} \\ \dfrac{\partial v}{\partial y} \\ \dfrac{\partial u}{\partial y} + \dfrac{\partial v}{\partial x}\end{Bmatrix}, \{\kappa\} = \begin{Bmatrix}\kappa_x \\ \kappa_y \\ \kappa_{xy}\end{Bmatrix} = \begin{Bmatrix}-\dfrac{\partial^2\theta}{\partial x^2} \\ -\dfrac{\partial^2\theta}{\partial y^2} \\ -2\dfrac{\partial^2\theta}{\partial x\,\partial y}\end{Bmatrix} \tag{10a}$$

$$\{\gamma^0\} = \begin{Bmatrix}\gamma_{xz}^0 \\ \gamma_{yz}^0\end{Bmatrix} = \begin{Bmatrix}\dfrac{\partial w}{\partial x} - \dfrac{\partial\theta}{\partial x} \\ \dfrac{\partial w}{\partial y} - \dfrac{\partial\theta}{\partial y}\end{Bmatrix} \tag{10b}$$

2.2 *Constitutive equations*

The linear elastic constitutive equations of FG-CNT sandwich plates can be written as:

$$\begin{aligned}\begin{Bmatrix}\sigma_x \\ \sigma_y \\ \sigma_{xy}\end{Bmatrix} &= \begin{bmatrix}Q_{11} & Q_{12} & Q_{16} \\ Q_{12} & Q_{22} & Q_{26} \\ Q_{61} & Q_{63} & Q_{66}\end{bmatrix}^k \begin{Bmatrix}\varepsilon_x \\ \varepsilon_y \\ \varepsilon_{xy}\end{Bmatrix} \\ \begin{Bmatrix}\sigma_{xz} \\ \sigma_{yz}\end{Bmatrix} &= \begin{bmatrix}Q_{55} & 0 \\ 0 & Q_{44}\end{bmatrix}^k \begin{Bmatrix}\gamma_{xz} \\ \gamma_{yz}\end{Bmatrix}\end{aligned} \tag{11}$$

where Q_{ij} is the stiffness coefficient matrix for each layer that k= 1, 2, and 3, defined as:

$$\begin{aligned}&Q_{11}^k = \frac{\mathrm{E}_{11}}{1-\nu_{12}\nu_{21}}, Q_{22}^k = \frac{\mathrm{E}_{22}}{1-\nu_{12}\nu_{21}}, Q_{12}^k = \frac{\nu_{21}\mathrm{E}_{11}}{1-\nu_{12}\nu_{21}}; \\ &Q_{44}^k = G_{23}, Q_{55}^k = G_{13}, Q_{66}^k = G_{12}, Q_{16}^k = Q_{26}^k = 0;\end{aligned} \tag{12}$$

For the homogeneous core, the shear modulus G is related to the Young's modulus by: $E = 2G(1+\nu)$. Based on Kelvin-Voigt's model on elastic materials with viscoelastic structural damping coefficient g, Young's moduli and shear modulus are substituted by the operator $\zeta = \zeta(1 + g\,\partial/\partial t)$ [26]. Thus, constitutive equations can be written in a new form as:

$$\begin{aligned}\begin{Bmatrix}\sigma_x \\ \sigma_y \\ \sigma_{xy}\end{Bmatrix} &= \begin{bmatrix}Q_{11} & Q_{12} & Q_{16} \\ Q_{12} & Q_{22} & Q_{26} \\ Q_{61} & Q_{63} & Q_{66}\end{bmatrix}^k \begin{Bmatrix}\varepsilon_x \\ \varepsilon_y \\ \varepsilon_{xy}\end{Bmatrix} + g\,\frac{\partial}{\partial t}\left(\begin{bmatrix}Q_{11} & Q_{12} & Q_{16} \\ Q_{12} & Q_{22} & Q_{26} \\ Q_{61} & Q_{63} & Q_{66}\end{bmatrix}^k \begin{Bmatrix}\varepsilon_x \\ \varepsilon_y \\ \varepsilon_{xy}\end{Bmatrix}\right) \\ \begin{Bmatrix}\sigma_{xz} \\ \sigma_{yz}\end{Bmatrix} &= \begin{bmatrix}Q_{55} & 0 \\ 0 & Q_{44}\end{bmatrix}^k \begin{Bmatrix}\gamma_{xz} \\ \gamma_{yz}\end{Bmatrix} + g\,\frac{\partial}{\partial t}\left(\begin{bmatrix}Q_{55} & 0 \\ 0 & Q_{44}\end{bmatrix}^k \begin{Bmatrix}\gamma_{xz} \\ \gamma_{yz}\end{Bmatrix}\right)\end{aligned} \tag{13}$$

2.3 Equations of motion

Hamilton's principle is used herein to derive equations of motion. The principle can be stated in an analytical form as:

$$0=\int_0^T\left(\delta U+\delta V-\delta K\right)dt \tag{14}$$

where δU , δV and δK are the variations of strain energy, work done, and kinetic energy, respectively. The variation of strain energy is given by:

$$\begin{aligned}&\delta U=\int_A\int_{-h/2}^{h/2}\left(\sigma_x\delta\varepsilon_x+\sigma_y\delta\varepsilon_y+\sigma_{xy}\delta\gamma_{xy}+\sigma_{xz}\delta\gamma_{xz}+\sigma_{yz}\delta\gamma_{yz}\right)dA\,dz=\int_A\left(\xi+g\frac{\partial\xi}{\partial t}\right)dA\\&\xi=N_x\frac{\partial\delta u}{\partial x}-M_x\frac{\partial^2\delta\theta}{\partial x^2}+N_y\frac{\partial\delta v}{\partial y}-M_y\frac{\partial^2\delta\theta}{\partial y^2}+N_{xy}\left(\frac{\partial\delta u}{\partial y}+\frac{\partial\delta v}{\partial x}\right)\\&-2M_{xy}\frac{\partial^2\delta\theta}{\partial x\,\partial y}+Q_x\left(\frac{\partial w}{\partial y}-\frac{\partial\theta}{\partial y}\right)+Q_y\left(\frac{\partial w}{\partial y}-\frac{\partial\theta}{\partial y}\right)\end{aligned} \tag{15}$$

where *N, M*, and *Q* are the stress resultants defined by

$$\left(N_x,N_y,N_{xy},M_X,M_Y,M_{XY}\right)=\int_{-h/2}^{h/2}\left(\sigma_x,\sigma_y,\sigma_{xy},z\,\sigma_x,z\,\sigma_y,z\,\sigma_{xy}\right)dz \tag{16a}$$

$$\left(Q_x,Q_y\right)=\int_{-h/2}^{h/2}\left(\sigma_{xz},\sigma_{yz}\right)dz \tag{16b}$$

Variations of work done by the viscoelastic foundation and transverse force can be written as:

$$\delta V=\int_A\left(\begin{array}{l}(k_w w-k_g\nabla^2 w+c\frac{\partial w}{\partial t}-q)\delta w+\\\left(N_x\frac{\partial w}{\partial x}\frac{\partial\delta w}{\partial x}+N_y\frac{\partial w}{\partial y}\frac{\partial\delta w}{\partial y}+2N_{xy}\frac{\partial w}{\partial x}\frac{\partial\delta w}{\partial y}\right)\end{array}\right)dA \tag{17}$$

where $k_w,k_g,c,q,N_x,N_y,N_{xy}$ are Winkler spring, Pasternak shear parameters, damping coefficient, distributed force acting on the top surface of the plate, and in-plane load, respectively. Finally, variation of kinetic energy can be written as:

$$\begin{aligned}&\delta K=\int_V\left(\dot{u}_1\delta\dot{u}_1+\dot{u}_2\delta\dot{u}_2+\dot{u}_3\delta\dot{u}_3\right)\rho(z)\,dA\,dz=\\&\int_A\left\{\begin{array}{l}I_0\left(\dot{u}\,\delta\dot{u}+\dot{v}\,\delta\dot{v}+\dot{w}\,\delta\dot{w}\right)-I_1\left(\dot{u}\frac{\partial\delta\dot{\theta}}{\partial x}+\frac{\partial\dot{\theta}}{\partial x}\delta\dot{u}+\dot{v}\frac{\partial\delta\dot{\theta}}{\partial y}+\frac{\partial\dot{\theta}}{\partial y}\delta\dot{v}\right)\\+I_2\left(\frac{\partial\dot{\theta}}{\partial x}\frac{\partial\delta\dot{\theta}}{\partial x}+\frac{\partial\dot{\theta}}{\partial y}\frac{\partial\delta\dot{\theta}}{\partial y}\right)\end{array}\right\}dA\end{aligned} \tag{18}$$

where $\rho(z)$ is the mass density, and (I_0,I_1,I_2) are mass inertias defined by:

$$\left(I_0, I_1, I_2\right) = \sum_{n=1}^{3} \int_{h_n-1}^{h_n} \left(1, z, z^2\right) \rho^{(n)}(z)\, dz \tag{19}$$

Substituting Eqs. (13), (15), and (16) into Eq. (12) the Hamilton principle by collecting $\delta u, \delta v, \delta w$ and $\delta\theta$ for viscoelastic sandwich plate is obtained as:

$$\delta u : N_{x,x} + N_{xy,y} - g\left(N_{x,xt} + N_{xy,yt}\right) = I_0 u_{,tt} - I_1 \theta_{,tx} \tag{20a}$$

$$\delta v : N_{xy,x} + N_{y,y} - g\left(N_{xy,xt} + N_{y,yt}\right) = I_0 v_{,tt} - I_1 \theta_{,ty} \tag{20b}$$

$$\begin{aligned} &\delta\theta : M_{x,xx} + 2M_{xy,xy} + M_{y,yy} - \left(Q_{x,x} + Q_{y,y}\right) - \\ &g\left(M_{x,xxt} + 2M_{xy,xyt} + M_{y,yyt} - \left(Q_{x,xt} + Q_{y,yt}\right)\right) = I_1\left(u_{,tx} + v_{,ty}\right) - I_2 \nabla^2 \theta_{,t} \end{aligned} \tag{20c}$$

$$\begin{aligned} &\delta w : Q_{x,x} + Q_{y,y} - g\left(Q_{x,xt} + Q_{y,yt} + w_{,t}\right) + q - k_w + \\ &k_g \nabla^2 w + c w_{,t} + N_x w_{,xx} + N_y w_{,yy} + 2N_{xy} w_{,xy} = I_0 w_{,tt} \end{aligned} \tag{20d}$$

By using of Eqs. (8), and (11) and substituting results into Eq. (16a) the axial forces N and bending moments M are obtained in terms of strains as:

$$\begin{Bmatrix} N_x \\ N_y \\ N_{xy} \\ M_x \\ M_y \\ M_{xy} \end{Bmatrix} = \begin{bmatrix} \begin{bmatrix} A_{11} & A_{12} & 0 \\ A_{12} & A_{22} & 0 \\ 0 & 0 & A_{66} \end{bmatrix} & \begin{bmatrix} B_{11} & B_{12} & 0 \\ B_{12} & B_{22} & 0 \\ 0 & 0 & B_{66} \end{bmatrix} \\ \begin{bmatrix} B_{11} & B_{12} & 0 \\ B_{12} & B_{22} & 0 \\ 0 & 0 & B_{66} \end{bmatrix} & \begin{bmatrix} D_{11} & D_{12} & 0 \\ D_{12} & D_{22} & 0 \\ 0 & 0 & D_{66} \end{bmatrix} \end{bmatrix} \begin{Bmatrix} \varepsilon_x^0 \\ \varepsilon_y^0 \\ \gamma_{xy}^0 \\ \kappa_x \\ \kappa_y \\ \kappa_{xy} \end{Bmatrix} \tag{21}$$

where A_{ij}, B_{ij}, D_{ij} are the stiffness coefficients defined by:

$$\left(A_{ij}, B_{ij}, D_{ij}\right) = \sum_{n=1}^{3} \int_{h_n-1}^{h_n} \left(1, z, z^2\right) Q_{ij}^{(n)}(z)\, dz \tag{22}$$

The in-plane stresses $\sigma_x, \sigma_y, \sigma_{xy}$ are obtained from constitutive equations as:

$$\{\sigma\} = [Q]\{\varepsilon\} = [Q]\left(\{\varepsilon^0\} + z\,\{\kappa\}\right) \tag{23}$$

The axial strain and the curvature are related to the axial forces N and bending moments M by the inversion of Eq. (21) as:

$$\begin{Bmatrix} \{\varepsilon^0\} \\ \{\kappa\} \end{Bmatrix} = \begin{bmatrix} [a] & [b] \\ [b] & [d] \end{bmatrix} \begin{Bmatrix} \{N\} \\ \{M\} \end{Bmatrix} \tag{24}$$

Substituting Eq. (24) into Eq. (23), the in-plane stresses can be rewritten as:

$$\{\sigma\} = [Q]\left\{\left([a] + z\,[b]\right)\{N\} + \left([b] + z\,[d]\right)\{M\}\right\} \tag{25}$$

In this theory σ_{xz}, σ_{yz} are obtained from equilibrium equation instead of constitutive equation that it should be used of correction factor because of the zero transverse shear stress conditions on the top and bottom surfaces of the plate. The equilibrium equations of a body are given by:

$$\frac{\partial \sigma_x}{\partial x} + \frac{\partial \sigma_{xy}}{\partial y} + \frac{\partial \sigma_{xz}}{\partial z} = 0 \tag{26a}$$

$$\frac{\partial \sigma_{xy}}{\partial x} + \frac{\partial \sigma_y}{\partial y} + \frac{\partial \sigma_{yz}}{\partial z} = 0 \tag{26b}$$

$$\frac{\partial \sigma_{xz}}{\partial x} + \frac{\partial \sigma_{yz}}{\partial y} + \frac{\partial \sigma_{zz}}{\partial z} = 0 \tag{26c}$$

The transverse shear stresses can be derived from Eq. (23) as:

$$\sigma_{xz} = -\int_{-h/2}^{z} \left(\frac{\partial \sigma_x}{\partial x} + \frac{\partial \sigma_{xy}}{\partial y} \right) dz \tag{27a}$$

$$\sigma_{yz} = -\int_{-h/2}^{z} \left(\frac{\partial \sigma_{xy}}{\partial x} + \frac{\partial \sigma_y}{\partial y} \right) dz \tag{27b}$$

Substituting Eq. (25) into Eq. (27) and omitting the weak terms, transverse shear stresses are obtained as [14]:

$$\sigma_{xz} = \varsigma(z) Q_x \tag{28a}$$

$$\sigma_{yz} = \xi(z) Q_y \tag{28b}$$

where

$$\varsigma = -\int_{-h/2}^{z} \left[Q_{11}(b_{11} + z d_{11}) + Q_{12}(b_{21} + z d_{21}) \right] dz \tag{29a}$$

$$\xi = -\int_{-h/2}^{z} \left[Q_{12}(b_{12} + z d_{12}) + Q_{22}(b_{22} + z d_{22}) \right] dz \tag{29b}$$

According to shear stresses defined in Eq. (28) the shear deformation energy per unit middle surface area is defined by:

$$\Pi_s = \frac{1}{2} \int_{-h/2}^{h/2} \sigma_{xz} \gamma_{xz} dz = \frac{1}{2} Q_x^2 \int_{-h/2}^{h/2} \frac{\varsigma^2(z)}{Q_{55}(z)} dz \tag{30}$$

where the average shear deformation energy per unit middle surface area is defined by:

$$\Pi_{sa} = \frac{1}{2} Q_x \gamma_{xy}^0 = \frac{1}{2} \frac{Q_x^2}{H_{55}} \tag{31}$$

where H_{55} is transverse shear stiffness that is obtained as:

$$T_{55}=\left(\sum_{n=1}^{3}\int_{h_{n-1}}^{h_n}\frac{\left[\varsigma^{(n)}(z)\right]^2}{Q_{55}^{(n)}(z)}dz\right)^{-1} \tag{32}$$

Similarly, the transverse shear stiffness H_{44} can be obtained as:

$$T_{44}=\left(\sum_{n=1}^{3}\int_{h_{n-1}}^{h_n}\frac{\left[\xi^{(n)}(z)\right]^2}{Q_{44}^{(n)}(z)}dz\right)^{-1} \tag{33}$$

Based on equilibrium equations the transverse shear forces are obtained as follow:

$$\begin{Bmatrix}Q_x\\Q_y\end{Bmatrix}=\begin{bmatrix}T_{55}&0\\0&T_{44}\end{bmatrix}\begin{Bmatrix}\gamma_{xz}^0\\\gamma_{yz}^0\end{Bmatrix} \tag{34}$$

Due to the isotropic properties of FG-CNT sandwich plates, $T_{55}=T_{44}=T$. Then, equations of motion of the new FSDT can be used in terms of displacements (*u, v, w, θ*) by substituting Eq. (10) into Eqs. (21) and (34) and the subsequent results into Eq. (20).

$$\begin{aligned}&A_{11}u_{,xx}+A_{66}u_{,yy}+(A_{12}+A_{66})v_{,xy}-B_{11}\theta_{,xxx}-(B_{12}+2B_{66})\theta_{,xyy}-g(A_{11}u_{,xxt}+A_{66}u_{,yyt}\\&+(A_{12}+A_{66})v_{,xyt}-B_{11}\theta_{,xxxt}-(B_{12}+2B_{66})\theta_{,xyyt})=I_0u_{,tt}-I_1\theta_{,ttx}\end{aligned} \tag{35a}$$

$$\begin{aligned}&A_{22}v_{,yy}+A_{66}v_{,xx}+(A_{12}+A_{66})u_{,xy}-B_{22}\theta_{,yyy}-(B_{12}+2B_{66})\theta_{,xxy}-g(A_{22}v_{,yyt}+A_{66}v_{,xxt}\\&+(A_{12}+A_{66})u_{,xyt}-B_{22}\theta_{,yyyt}-(B_{12}+2B_{66})\theta_{,xxyt})=I_0v_{,tt}-I_1\theta_{,tty}\end{aligned} \tag{35b}$$

$$\begin{aligned}&B_{11}u_{,xxx}+(B_{12}+2B_{66})u_{,xyy}+(B_{12}+2B_{66})v_{,xxy}+B_{22}v_{,yyy}-D_{11}\theta_{,xxxx}-2(D_{12}+2D_{66})\theta_{,xxyy}\\&-D_{22}\theta_{,yyyy}-H\nabla^2w+H\nabla^2\theta-g(B_{11}u_{,xxxt}+(B_{12}+2B_{66})u_{,xyyt}+(B_{12}+2B_{66})v_{,xxyt}\\&+B_{22}v_{,yyyt}-D_{11}\theta_{,xxxxt}-D_{22}\theta_{,yyyyt}-2(D_{12}+2D_{66})\theta_{,xxyyt}-H\nabla^2w_{,t}+H\nabla^2\theta_{,t})=I_1(u_{,ttx}+v_{,tty})-I_2\nabla^2\theta_{,tt}\end{aligned} \tag{35c}$$

$$\begin{aligned}&H\nabla^2w-H\nabla^2\theta+q-k_w+k_g\nabla^2w+cw_{,t}+N_xw_{,xx}+N_yw_{,yy}+2N_{xy}w_{,xy}-g(H\nabla^2w_{,t}-H\nabla^2\theta_{,t}\\&+q-k_w+k_g\nabla^2w_{,t}+cw_{,tt}+N_xw_{,xxt}+N_yw_{,yyt}+2N_{xy}w_{,xyt})=I_0w_{,tt}\end{aligned} \tag{35d}$$

3 ANALYTICAL SOLUTION

In this section, governing equation of viscoelastic sandwich plates with homogeneous core and FG-CNT reinforced facesheets is solved with supposing of the following expansions of generalized displacements.

$$\begin{aligned}u(x,y,t)&=U_{mn}\sin(\alpha x)\sin(\beta y)e^{i\omega t}\\v(x,y,t)&=V_{mn}\sin(\alpha x)\sin(\beta y)e^{i\omega t}\\w(x,y,t)&=W_{mn}\sin(\alpha x)\sin(\beta y)e^{i\omega t}\\\theta(x,y,t)&=\theta_{mn}\sin(\alpha x)\sin(\beta y)e^{i\omega t}\end{aligned} \tag{36}$$

where $i=\sqrt{-1}$, $U_{mn},V_{mn},W_{mn},\theta_{mn}$ are coefficients and ω is the natural frequency, and $\alpha=m\pi/a,\beta=n\pi/b$. The transversely load q is supposed as:

$$q\left(x,y\right)=Q_{mn}\sin(\alpha x)\sin(\beta y) \tag{37}$$

where the coefficient Q_{mn} is given q_0 for sinusoidal load. By substituting Eqs. (37) and (36) into Eq. (35) the analytical solution can be obtained as:

$$\left(K+i\,\omega C-\omega^2 M\right)\begin{Bmatrix}U_{mn}\\V_{mn}\\\theta_{mn}\\W_{mn}\end{Bmatrix}=\begin{Bmatrix}0\\0\\0\\q_0\end{Bmatrix} \tag{38a}$$

$$K=\begin{bmatrix}K_{11} & K_{12} & K_{13} & 0\\ K_{21} & K_{22} & K_{23} & 0\\ K_{31} & K_{32} & K_{33} & K_{34}\\ 0 & 0 & K_{43} & K_{44}+\lambda\end{bmatrix},C=gK-\begin{bmatrix}0 & 0 & 0 & 0\\ 0 & 0 & 0 & 0\\ 0 & 0 & 0 & 0\\ 0 & 0 & 0 & \chi\end{bmatrix},$$
$$M=\begin{bmatrix}M_{11} & 0 & M_{13} & 0\\ 0 & M_{22} & M_{23} & 0\\ M_{31} & M_{32} & M_{33} & M_{34}\\ 0 & 0 & 0 & M_{44}\end{bmatrix},\chi=c-k_w-k_g(\alpha^2+\beta^2) \tag{38b}$$

where λ , [*M*], [*C*] and [*K*] denote coefficient of critical buckling load, mass matrix, damping matrix and stiffness matrix, respectively.

By substituting $\lambda=0$ and $\left[M\right]=0$ in Eq. (38a) and if the determinant of coefficient of Eq. (38a) set to zero, the deflection of viscoelastic sandwich plate will be obtained. Also by assuming $q=0$ and $\left[M\right]=0$ in Eq. (38a) and if the determinant of coefficient of Eq. (38a) set to zero, the critical buckling load of viscoelastic sandwich plate will be obtained. For the free vibration analysis of viscoelastic sandwich plate, it is convenient to rewrite the coefficients of Eq. (38a) in form as follows:

$$\left[\Lambda\right]=\begin{bmatrix}[0] & [I]\\ -[M]^{-1}[K] & -[M]^{-1}[C]\end{bmatrix} \tag{39}$$

where $[I]$ is the unitary matrix. The free vibration of viscoelastic sandwich plate will be obtained by supposing $q=\lambda=0$ in Eq. (38) and the determinant of coefficient of Eq. (39) set to zero.

In this study, only simply supported boundary condition is considered and is as follows:

$$\begin{aligned}&N_x=v=\theta=w=M_x=0 \qquad at\ x=0,a\\ &u=N_y=\theta=w=M_y=0 \qquad at\ y=0,b\end{aligned} \tag{40}$$

where *a* and *b* refer to the length and width of the plate, respectively.

4 NUMERICAL RESULTS AND DISCUSSION

In this section, first, the accuracy of the present formulation is investigated through example of elastic sandwich plates with carbon nanotubes (CNTs) reinforced composite facesheets. Then, a parametric study is carried out to show the effects of the viscoelastic parameter in the free vibration characteristics of the viscoelastic sandwich plates. In addition, in this theory, the result is estimated near to HSDT or SSDT [14]. For the present study, four different core-to-facesheet thickness ratios h_c/h_f , three thickness ratios a/h , and two dimension ratios a/b are considered.

In this case, we take Polymethyl methacrylate (PMMA) as the matrix in which the CNTs are used as reinforcements. The materials properties of which are assumed to be: mass density, $\rho_m = 1150 kg/m^3$, Poisson's ratio, $\upsilon_m = 0.34$,and Young's modulus, $E_m = 2.1 Gpa$. Single walled CNTs are used as reinforcements and the material properties are given in Table 1. The following CNT efficiency parameters are used [28]: $\eta_1 = 0.137$, $\eta_2 = 1.002$ and $\eta_3 = 0.175$ for $V^*_{CNT} = 0.12$; $\eta_1 = 0.142$, $\eta_2 = 1.626$, and $\eta_3 = 1.138$ for $V^*_{CNT} = 0.17$ or $\eta_1 = 0.149$, $\eta_2 = 1.381$, and $\eta_3 = \eta_2$ for $V^*_{CNT} = 0.17$ that it is assumed for this study; $\eta_1 = 0.141$, $\eta_2 = 1.585$ and $\eta_3 = 1.109$ for $V^*_{CNT} = 0.28$, and also we assume $G_{12} = G_{13} = G_{23}$. For the homogeneous core, we use Ti-6Al-4V Titanium alloy. The properties are: $E_c = 102.6982 Gpa$, $\upsilon_c = 0.29$, and $\rho_c = 4429 kg/m^3$ [24]. For convenience, the following non-dimensional forms are used:

$$\overline{w} = \frac{E_c h^3}{q_0 a^4} w\left(\frac{a}{2}, \frac{b}{2}\right), \quad \overline{N} = \frac{N_{cr} a^2}{100 E_c h^3}, \quad \overline{\omega} = \omega \frac{a^2}{h}\sqrt{\frac{\rho_c}{E_c}}, \quad \overline{\sigma}_{xx} = \frac{h^2}{q_0 a^2}\sigma_{xx}\left(\frac{a}{2}, \frac{b}{2}, z\right) \tag{41}$$

Table 1
Material properties depended on temperature for (10, 10) SWCNT (R=0.68nm, L=9.26nm, h=0.067nm, $\rho = 1400 kg/m^3$, $v_{12} = 0.175$ [27].

Temperature(K)	$E_{11}^{CNT}(TPa)$	$E_{22}^{CNT}(TPa)$	$G_{12}^{CNT}(TPa)$	$\alpha_{12}^{CNT}(1/GPa.K)$	$\alpha_{22}^{CNT}(1/GPa.K)$
300	5.6466	7.08	1.9445	3.4584	5.1682
500	5.5308	6.9348	1.9643	4.5361	5.0189
700	5.4744	6.8641	1.9644	4.6677	4.8943

The first analysis discuses about the bending responses of FG-CNT sandwich plates for all type of FG-CNT distribution of nanotubes in facesheets. In Fig. 2, variations of bending parameter versus thickness ratios are presented for different kind of FG-CNT distribution of nanotubes in facesheets. It is clear that the FG-X is more stiffness than other models because of excessive distribution of nanotubes in facesheets edges. For verifying the accuracy of the present study, the obtained result of the bending responses of FG-CNT sandwich plates are compared with those generated by Natarajana, [24], based on omitting of viscoelastic parameter of materials and foundation and good agreement between the results is found as shown in Table 2. Moreover, it can be seen that non-dimensionalized bending ($\overline{w}$) of the sandwich plate decreases with increasing of the plate thickness, CNT volume fraction, and the core-to-facesheet thickness.

Table 2
Dimensionless deflections ($\overline{w}$) of sandwich plates with homogeneous core and CNT reinforced facesheets for two volume fraction of CNTs distribution.

a	a/h	h_c/h_f	FG-X		UD			
			$V^*_{CNT} = 0.17$	$V^*_{CNT} = 0.28$	$V^*_{CNT} = 0.17$		$V^*_{CNT} = 0.28$	
					Present	[24]	Present	[24]
1	5	1	0.098989	0.082078	0.116142	-	0.093934	-
		2	0.074298	0.060651	0.082708	0.0813	0.070642	0.0659
		6	0.041302	0.035075	0.048023	0.0504	0.041828	0.0441
		10	0.034784	0.029923	0.040255	-	0.035827	-
	10	1	0.044466	0.033126	0.060777	-	0.044037	-
		2	0.039103	0.028730	0.052846	0.0658	0.039610	0.0485
		6	0.031507	0.024612	0.040575	0.0461	0.033379	0.0391
		10	0.029927	0.024540	0.036378	-	0.031637	-
	20	1	0.030836	0.023194	0.046936	-	0.031852	-
		2	0.030304	0.021996	0.045381	-	0.031562	-
		6	0.029058	0.020888	0.038713	-	0.031267	-
		10	0.028713	0.020750	0.035408	-	0.030589	-

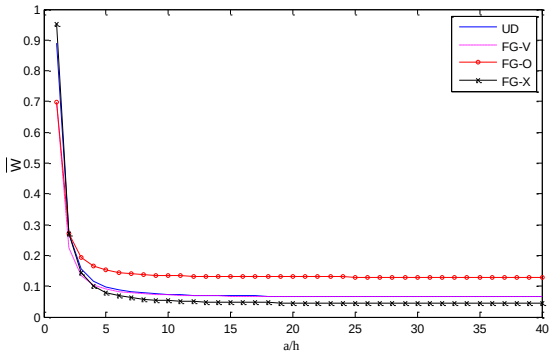

Fig.2
Comparison of dimensionless deflection ($\bar{w}$) of sandwich plate with different functionally graded distribution of CNTs in the facesheets for $V^*_{CNT} = 0.17$ and $h_c = 2h_f$.

In Fig. 3, variations of the non-dimensionalized natural frequency ($\bar{\omega}$) of FG-CNT sandwich plates versus thickness ratios are presented for $V^*_{CNT} = 0.17$ in all type of FG-CNT distribution of nanotubes in facesheets. It can be observed that the natural frequency of FG-X is the highest in all type of distribution again. By neglecting of viscoelastic parameters for verifying the accuracy of the present study, the results of natural frequency are tabulated in Table 3. It can be opined that non-dimensionalized natural frequency ($\bar{\omega}$) increases with increasing CNT volume fraction and the core-to-facesheet thickness ratios and increases with decreasing of sandwich plate thickness.

Table 3
Non-dimensionalized natural frequency ($\bar{\omega}$) of sandwich plates with homogeneous core and CNTs reinforced facesheets for two types of CNTs distribution.

a/b	a/h	h_c/h_f	UD		FG-X			
			$V^*_{CNT} = 0.17$	$V^*_{CNT} = 0.28$	$V^*_{CNT} = 0.17$		$V^*_{CNT} = 0.28$	
					Present	[24]	Present	[24]
1	5	1	3.465808	3.773022	3.881289	-	4.083990	-
		4	3.706537	3.937642	4.495638	-	4.686465	-
		6	4.522709	4.685133	4.775714	4.7512	4.967339	5.0871
		10	4.807927	4.950888	5.031100	-	5.221526	-
	10	1	4.088209	4.583354	4.829541	-	5.342312	-
		4	4.118581	4.703114	4.925100	-	5.442312	-
		6	4.768067	4.994028	5.107724	5.0895	5.455984	5.5223
		10	5.079717	5.233136	5.320693	-	5.563700	-
	20	1	4.247947	4.913319	4.985125	-	5.479573	-
		4	4.308636	5.073246	5.056681	-	5.559837	-
		6	4.837750	5.083771	5.204892	5.1886	5.588221	5.6534
		10	5.157394	5.313885	5.403658	-	5.663309	-

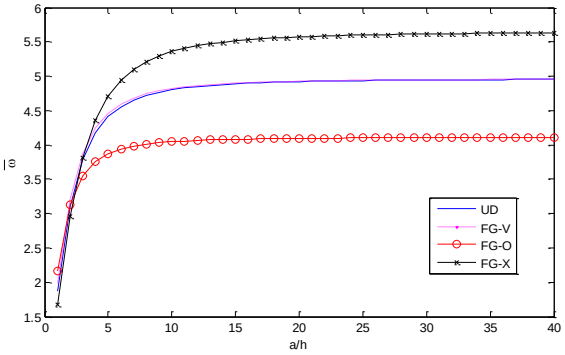

Fig.3
Comparison of non-dimensionalized natural frequency ($\bar{\omega}$) of sandwich plate with different functionally graded distribution of CNTs in the facesheets for $V^*_{CNT} = 0.17$ and $h_c = 2h_f$.

In Fig.4, variations of the non-dimensionalized critical buckling load ($\bar{N}$) of FG-CNT sandwich plates versus thickness ratios in absence of viscoelastic parameter of materials and foundation are presented for $V^*_{CNT} = 0.17$ in all

type of FG-CNT distribution of nanotubes in facesheets. Then, the maximum critical buckling load is related to FG-X, the minimum critical buckling load is related to FG_O, and UD,FG-V are the same as each other. In Table 4, the results of the non-dimensionalized critical buckling load for two types of UD and FG-X are tabulated. It can be seen that critical buckling load increases with increasing of CNT volume fraction and the core-to-facesheet thickness and increases with decreasing of sandwich plate thickness.

Table 4

Non-dimensionalized critical buckling load ($\bar{N}$) of sandwich plates with homogeneous core and CNT reinforced facesheets for two volume fraction of CNTs distribution.

a/b	a/h	h_c/h_f	UD		FG-X	
			$V^*_{CNT}=0.17$	$V^*_{CNT}=0.28$	$V^*_{CNT}=0.17$	$V^*_{CNT}=0.28$
1	5	1	0.521657	0.554679	0.629263	0.652391
		2	0.731164	0.740902	0.824412	0.882877
		6	1.163730	1.269278	1.390385	1.526614
		10	1.361646	1.488923	1.605029	1.789512
	10	1	0.956422	1.199943	1.334737	1.616445
		2	1.087296	1.339823	1.490138	1.863785
		6	1.356021	1.601126	1.770854	2.175627
		10	1.495996	1.691572	1.836793	2.182015
	20	1	1.208151	1.679169	1.854518	2.308605
		2	1.238053	1.692033	1.867057	2.434358
		6	1.414451	1.713097	1.900895	2.563470
		10	1.533831	1.751156	1.905584	2.580556

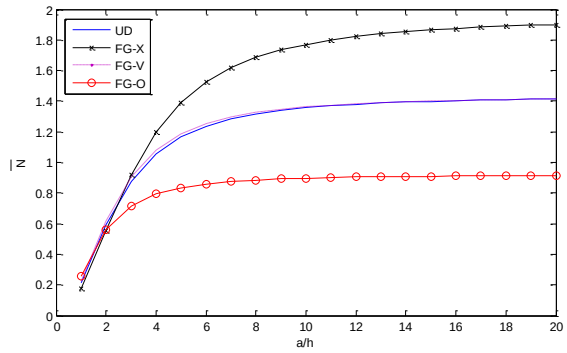

Fig.4
Comparison of non-dimensionalized critical buckling load ($\bar{N}$) of sandwich plate with different functionally graded distribution of CNTs in the facesheets for $V^*_{CNT}=0.17$ and $h_c=2h_f$.

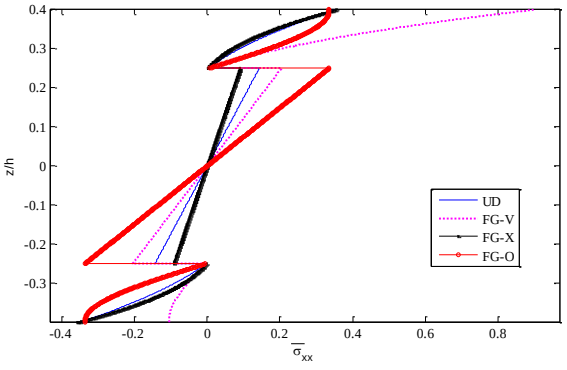

Fig.5
Non-dimensionalized stress in x direction ($\bar{\sigma}_{xx}$) of sandwich plate versus thickness with different functionally graded distribution of CNTs in the facesheets for $V^*_{CNT}=0.17$ and $h_c=4h_f$.

In Fig. 5, through thickness variation of stresses in all type of square FG-CNT sandwich plate for with $h_c=4h_f$ and a/h = 5 and is demonstrated. A significant difference in the through thickness non-dimensionalized stresses are related to FG-X and FG-O. It can be seen that, FG-V type behavior different in top and bottom of facesheets because the distribution of CNTs is not symmetry. In other words, the volume fractions of CNTs in bottom edges of both facesheets are closed to zero.

After representing the accuracy of the formulation, parametric study of the frequency for the viscoelastic sandwich plates is presented. For numerical results, the following parameters for material of viscoelastic sandwich plates and viscoelastic foundation are considered [9-29]:

$k_g = 2.071273\ N/m$, $k_w = 8.9995035\ TN/m$, $c = 1*10^7\ pa.s$, and $g = 1*10^{-10}\ s$

In Table 5., variations of dimensionless frequency of viscoelastic sandwich plate for all types of FG-CNTs reinforced composite facesheets on viscoelastic foundation are tabulated. As expected, the ratios of frequency in viscoelastic medium have been exceedingly decreased and still frequency of FG-X distribution is higher than other types of FG-CNTs distribution. It can be seen that by increasing core-to-facesheet thickness ratios and decreasing of sandwich plate thickness, non-dimensionalized frequency ($\bar{\omega}$) will be increased. Fig. 6 depicted the non-dimensionalized frequency ($\bar{\omega}$) versus viscoelastic structural damping coefficient (g) for various FG-CNTs distribution, $V^*_{CNT} = 0.17$, and $h_c = 2h_f$. It can be observed that ($\bar{\omega}$) decreases by increasing (g) and for $g \geq 0.5*10^{-4}$, viscoelastic structural damping coefficient effect on the ($\bar{\omega}$) is same for all types of FG-CNTs distribution.

Table 5
Non-dimensionalized frequency ($\bar{\omega}$) of viscoelastic sandwich plates based on viscoelastic foundation with CNTs reinforced facesheets for all types of CNTs distribution and $V^*_{CNT} = 0.17$.

a/b	a/h	h_c/h_f	FG-O	UD	FG-V	FG-X
1	5	1	0.007987	0.010461	0.013476	0.011680
		4	0.017368	0.020341	0.022139	0.022504
		6	0.022361	0.025658	0.026895	0.028041
		10	0.030116	0.033894	0.034510	0.036564
	10	1	0.009993	0.014716	0.016433	0.017526
		4	0.018742	0.024184	0.024893	0.028319
		6	0.024179	0.029401	0.029858	0.033603
		10	0.033216	0.038004	0.038229	0.042040
	20	1	0.010750	0.016814	0.017406	0.020916
		4	0.019015	0.025260	0.025474	0.030176
		6	0.024496	0.030243	0.030381	0.035024
		10	0.033768	0.038728	0.038801	0.043092

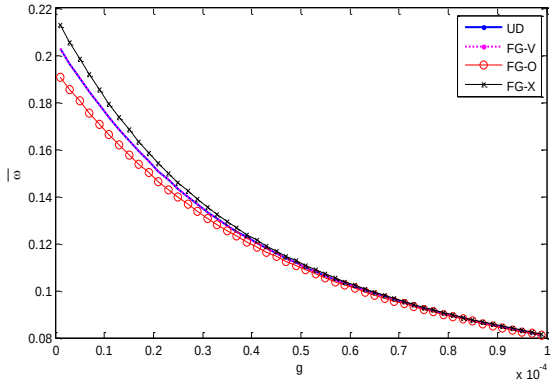

Fig.6
Non-dimensionalized frequency ($\bar{\omega}$) of sandwich plate versus viscoelastic structural damping coefficient (g) with different functionally graded distribution of CNTs in the facesheets for $V^*_{CNT} = 0.17$ and $h_c = 2h_f$.

Fig. 7 depicted dimensionless frequency ($\bar{\omega}$) of viscoelastic structural sandwich plate to thickness ratios (a/h) for various FG-CNTs distribution in the facesheets, $V^*_{CNT} = 0.17$, and $h_c = 2h_f$. It can be seen that $\bar{\omega}$ increases with an increase in a/h. In addition, as it is mentioned in above, frequency of FG-X distribution is higher than other types of FG-CNTs distribution. $\bar{\omega}$ is tended to constant value at $a/h \geq 11$ for other types of CNTs distribution.

In Fig. 8, Non-dimensionalized frequency ($\bar{\omega}$) of viscoelastic sandwich plate to core-to-facesheet thickness ratios (h_c / h_f) is demonstrated for various length to width ratios (*a/b*) for UD distribution, $V^*_{CNT} = 0.28$, and $a = 20h$. It is clear that $\bar{\omega}$ increases by increasing of (h_c / h_f) and for $a/b > 1$, $\bar{\omega}$ will be increased, for $a/b < 1$, $\bar{\omega}$ will be decreased.

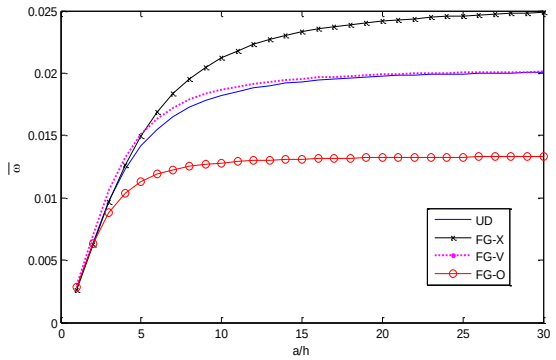

Fig.7
Non-dimensionalized frequency ($\bar{\omega}$) of viscoelastic sandwich plate versus thickness ratios with different functionally graded distribution of CNTs in the facesheets for $V^*_{CNT} = 0.17$ and $h_c = 2h_f$.

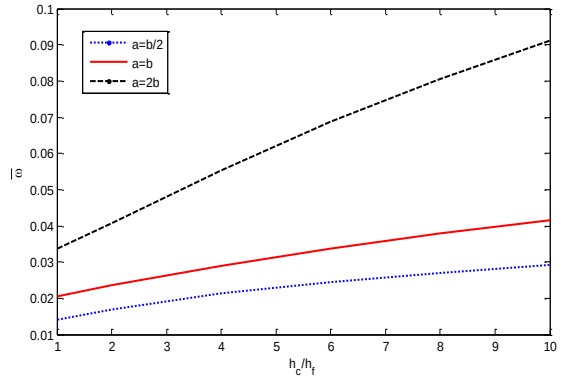

Fig.8
Non-dimensionalized frequency ($\bar{\omega}$) of viscoelastic sandwich plate versus core-to-facesheet thickness ratios for UD distribution, $V^*_{CNT} = 0.28$, and $a = 20h$.

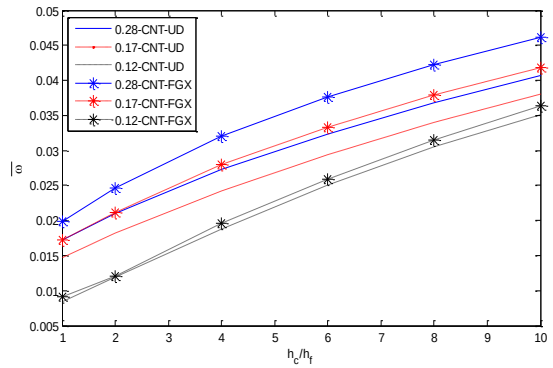

Fig.9
Non-dimensionalized frequency ($\bar{\omega}$) of viscoelastic sandwich plate versus core-to-facesheet thickness ratios for $a = b$, and $a = 10h$.

Fig. 9 shows the variations of Non-dimensionalized frequency ($\bar{\omega}$) with increasing of core-to-facesheet thickness ratios for two cases of CNTs distribution with different volume fraction of CNTs. The Non-dimensionalized frequency is changed with respect to the core-to-facesheet thickness ratios and the frequencies with increasing the volume fraction of CNTs and those distributions are increased. Moreover, in the lower volume fraction of CNTs, differences of frequencies are very low between types of CNTs distribution.

Finally, the variation of the non-dimensionalized frequency ($\bar{\omega}$) with increasing of damping coefficient (*c*) is plotted in Fig.10. This diagram is depicted for various FG-CNTs distribution with $V^*_{CNT} = 0.17$ and $h_c = 2h_f$. It is clear that non-dimensionalized frequency decreases by increasing of damping coefficient and the frequencies tend to the constant value with increasing of damping coefficient.

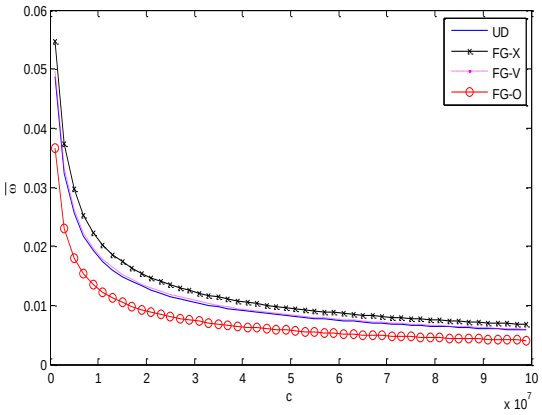

Fig.10
Non-dimensionalized frequency ($\bar{\omega}$) of sandwich plate versus damping coefficient (c) with different functionally graded distribution of CNTs in the facesheets for $V^{*}_{CNT} = 0.17$ and $h_c = 2h_f$.

5 CONCLUSION

The vibration analysis of the viscoelastic sandwich plates was investigated based on new first order shear deformation theory and Kelvin–Voigt model. Verification studies confirm that the new FSDT is more accurate than the conventional one which the number of unknowns and governing equations are reduced. After deriving the equation of motion, the analytical method was used to solve the problem. Considering the various parameters such as the sandwich type, the thickness ratio and the volume fraction of the CNTs with the structural damping and viscoelastic foundation is the main contributions of the present paper. Based on the numerical results, the following main conclusions are drawn. It was found that the volume fraction of the CNTs, FG-CNTs distribution, the structural damping, core-to-facesheet thickness ratios, stiffness and damping of the foundation are affected on the stability of viscoelastic sandwich plate. Moreover, the frequency decreases with using foundation, increasing the viscoelastic structural damping coefficient, and increasing damping coefficient of materials and foundation.

ACKNOWLEDGMENTS

The author would like to thank the reviewers for their comments and suggestions to improve the clarity of this article. Iranian Nanotechnology Development Committee provided financial support. This work was also supported by University of Kashan [grant number 574600/1].

REFERENCES

[1] Vinson J.R., 2001, Sandwich structures, *Apply Mechanic* **54**: 201-214.
[2] Sun C.H., Li F., Cheng H.M., Lu G.Q., 2005, Axial Young's modulus prediction of single walled carbon nanotube arrays with diameters from nanometer to meter scales, *Apply Physics* **87**:193-201.
[3] Jia J., Zhao J., Xu G., Di J., Yong Z., TaoY., Fang C., Zhang Z., Zhang X., Zheng L., 2011, A comparison of the mechanical properties of fibers spun from different carbon nanotubes, *Carbon* **49**: 1333-1339.
[4] Whitney J., 1972, Stress analysis of thick laminated composite and sandwich plates, *Journal of Composite Materials* **6**: 426-440.
[5] Zenkour A., 2005, A comprehensive analysis of functionally graded sandwich plates: Part 1 - deflection and stresses, *International Journal of Solids and Structures* **42**: 5224-5242.
[6] Ugale V., Singh K., Mishra N., 2013, Comparative study of carbon fabric reinforced and glass fabric reinforced thin sandwich panels under impact and static loading, *Composite Materials* **49**: 99-112.
[7] Thostenson E., Chou T-W., 2002, Aligned multi-walled carbon nanotube-reinforced composites, *Processing and Mechanical Characterization, Apply Physics* **35**: L77.
[8] Zhu P., Lei Z., Liew K., 2012, Static and free vibration analyses of carbon nanotube-reinforced composite plates using finite element method with first order shear deformation plate theory, *Composite Structure* **94**: 1450-1460.
[9] Mohammadimehr M., Navi B., Arani A., 2014, Biaxial buckling and bending of smart nanocomposite plate reinforced by cnts using extended mixture rule approach, *Mechanics of Advanced Composite Structures* **1**: 17-26.

[10] Arani A., Maghamikia S., Mohammadimehr M., Arefmanesh A., 2011, Buckling analysis of laminated composite rectangular plates reinforced by SWCNTs using analytical and finite element methods, *Journal of Mechanical Science and Technology* **25**: 809-820.

[11] Arani A., Jafari G-S., 2015, Nonlinear vibration analysis of laminated composite mindlin micro/nano-plates resting on orthotropic pasternak medium using DQM, *Advances in Applied Mathematics and Mechanics* **36**: 1033-1044.

[12] ZenkourA., Sobhy M., 2010, Thermal buckling of various types of FGM sandwich plates, *Composite Structures* **93**: 93-102.

[13] Sobhy M., 2013, Buckling and free vibration of exponentially graded sandwich plates resting on elastic foundations under various boundary conditions, *Composite Structures* **99**: 76-87.

[14] Thai H-T., Nguyen T-K., Thuc P., Lee J., 2014, Analysis of functionally graded sandwich plates using a new first-order shear deformation theory, *European Journal of Mechanics A/Solids* **45**: 211-225.

[15] Zhang L.W., Lei Z.X., Liew K.M., 2015, An element-free IMLS-Ritz framework for buckling analysis of FG–CNT reinforced composite thick plates resting on Winkler foundations, *Engineering Analysis with Boundary Elements* **58**: 7-17.

[16] Shen H-S., 2009, Nonlinear bending of functionally graded carbon nanotube- reinforced composite plates in thermal environments, *Composite Structures* **91**: 9-19.

[17] Lei Z.X., Liew K.M., Yu J.L., 2013, Large deflection analysis of functionally graded carbon nanotubes reinforced composite plates by the element-free kp-Ritz method, *Computer Methods in Applied Mechanics and Engineering* **256**: 89-99.

[18] Zhang L.W., Lei Z.X., Liew K.M., Yu J.L., 2014, Largedeflection geometrically nonlinear analysis of carbon nanotubes reinforced functionally graded cylindrical panels, *Computer Methods in Applied Mechanics and Engineering* **273**: 1-18.

[19] Lei Z.X., Liew K.M., Yu J.L., 2013, Buckling analysis of functionally graded carbon nanotube-reinforced composite plates using the element-free kp-Ritz method, *Composite Structures* **98**: 160-168.

[20] Lei Z.X., Zhang L.W., Liew K., Yu J.L., 2013, Dynamic stability analysis of carbon nanotubes reinforced functionally graded cylindrical panels using the element- free kp-Ritz method, *Composite Structures* **113**: 328-338.

[21] Srivastava I., Yu Z.Z., Koratkar N.A., 2012, Viscoelastic properties of graphene–polymer composites, *Advanced Science, Engineering and Medicine* **4**: 10-14.

[22] Su Y., Wei H., Gao R., Yang Z., Zhang J., Zhong Z., 2012, Exceptional negative thermal expansion and viscoelastic properties of graphene oxide paper, *Carbon* **50**: 2804-2809.

[23] Pouresmaeeli S., Ghavanloo E., Fazelzadeh S.A., 2013, Vibration analysis of viscoelastic orthotropic nanoplates resting on viscoelastic medium, *Composite Structures* **96**: 405-410.

[24] Natarajana S., Haboussib M., Ganapathic M., 2014, Application of higher-order structural theory to bending and free vibration analysis of sandwich plates with CNT reinforced composite facesheets, *Composite Structures* **113**: 197-207.

[25] Malekzadeh P., Shojaee M., 2013, Buckling analysis of quadrilateral laminated plates with carbon nanotubes reinforced composite layers, *Thin-Walled Structures* **71**: 108-118.

[26] Drozdov A.D., 1998, *Viscoelastic Structures: Mechanics of Growth and Aging*, San Diego, Academic Press.

[27] Shen H-S., Zhang C-L., 2010, Thermal buckling and postbuckling behavior of functionally graded carbon nanotube-reinforced composite plates, *Materials and Design* **31**: 3403-3411.

[28] Wang Z-X., Shen H-S., 2012, Nonlinear vibration and bending of sandwich plates with nanotube reinforced composite, *Composites Part B: Engineering* **43**: 411-421.

[29] Ghavanloo E., Fazelzadeh S. A., 2011, Flow-thermoelastic vibration and instability analysis of viscoelastic carbon nanotubes embedded in viscous fluid, *Physica E* **44**: 17-24.